TECHNICAL PAPER

JOURNAL OF THE SOUTH AFRICAN INSTITUTION OF CIVIL ENGINEERING

Vol 51 No 1, 2009, Pages 15–25, Paper 689

Experimentally applied earthquakes and associated loading on a full-scale dry-stacked masonry structure

A Elvin

This paper describes some practical aspects of testing full-scale structures under realistic earthquake loading. A method of filtering earthquake signals so that they can be applied by servo-hydraulic test machines with limited displacement capabilities is presented. Two standard high-pass filtering methods, the moving average and the 4th order Butterworth, are considered. Both filters produce very similar results. The El Centro, Northridge and Llolleo earthquakes are considered as case studies. They were filtered and applied to a shaking table carrying a full-scale dry-stacked masonry structure. The table's displacements and accelerations were measured and compared with the filtered curves. The measured displacements showed good agreement with the filtered earthquake signal. The error in the actual applied (measured) accelerations was much greater due to the fact that the tests were carried out in displacement (not acceleration) control, and to the testing system noise (around 13 Hz). The response spectra for the filtered, unfiltered and measured accelerations for the three earthquakes were computed and compared with design earthquake spectra. It was found that at the natural period of the test structure considered, the response spectrum from the original earthquake accelerations and from the filtered/applied accelerations were almost the same.

INTRODUCTION

Ground motion is relatively rare in South Africa, with most seismic activity being associated with mine tremors. However, these earth tremors can be larger than 5,0 on the Richter scale (see Saunders 2005 for a list of such events since 1960). As the South African structural industry expands and starts to build in other parts of the world, seismic-resistant structural design will become critical. Although the performance of reinforced concrete and steel structures in seismic zones is relatively well understood, the performance of masonry structures is still a largely unsolved problem. The now common use of dry-stacked brick structures as a low-cost housing solution in South Africa might provide an attractive alternative for the international housing market. However, many of these markets, such as in South America, are located in severe earthquake regions.

A dry-stacked brick structure is defined as one in which mortar is not used to bind the bricks. The bricks are held together using a lock-and-key-type mechanism (see Hydraform 2009 for a comprehensive summary of such systems). This makes construction relatively simple and inexpensive. However, the analytical design of dry-stacked brick structures is complicated for a number of reasons, including the non-linear behaviour of the friction and keys between the bricks. Therefore several research groups have been investigating the performance of masonry structures experimentally. These tests have typically been performed on small-scale models or structural components such as single walls (e.g. Griffith et al 2004). Ngowi (2006) and Mofana and Rathebe (2005), on the other hand, considered a full-scale single-story dry-stacked house subjected to pure harmonic base excitation.

In this paper the experimental techniques that can be used to load large structures seismically under realistic earthquake loading are presented. Special emphasis is placed on overcoming the limitations of the test equipment. Tests performed on a full-scale single-story dry-stack building, similar to those described by Ngowi (2006) and Mofana and Rathebe (2005), are used to illustrate the techniques.

The organisation of this paper is as follows: first, the three test earthquakes to be used are identified and the earthquake testing equipment is described. Next, the acceleration signals are double-integrated to produce the displacement time history. The procedure for filtering the displacement history is presented, and the resulting signal double-differentiated and compared with the original accelerations. After an explanation of how earthquake response spectra are obtained, the response spectra for the three test earthquakes are computed and compared against several design

ALEX ELVIN graduated from the Department of Civil Engineering, University of the Witwatersrand, in 1989. He completed his Master's in 1991 and his PhD in 1996, both at the Massachusetts Institute of Technology (MIT). He has worked in industry and taught several classes at MIT. He was a junior faculty member at Harvard Medical School from 1998 to 2002 doing finite element analysis of implants. Since 2007 he has been an Associate Professor in Structural Mechanics at the University of the Witwatersrand. His research interests are theoretical (numerical) modelling, SMART materials, instrumentation and sensor networks in engineering, and health monitoring of structures.

Contact details:
School of Civil and Environmental Engineering
University of the Witwatersrand
Johannesburg
T 011-717-7145
F 011-717-7045
alex.elvin@wits.ac.za

Keywords: earthquake testing, filtering, full-scale testing, earthquake response spectra

***Table 1** Statistics of the three earthquakes*

Earthquake	Year	PGA (g)	Length of record (s)	Magnitude Richter scale
El Centro	1940	0,3	31	7,1
Northridge	1994	0,3	28	6,7
Llolleo	1985	0,7	116	7,8

Note: PGA stands for peak ground acceleration, typically measured in g (9,8 m/s^2)

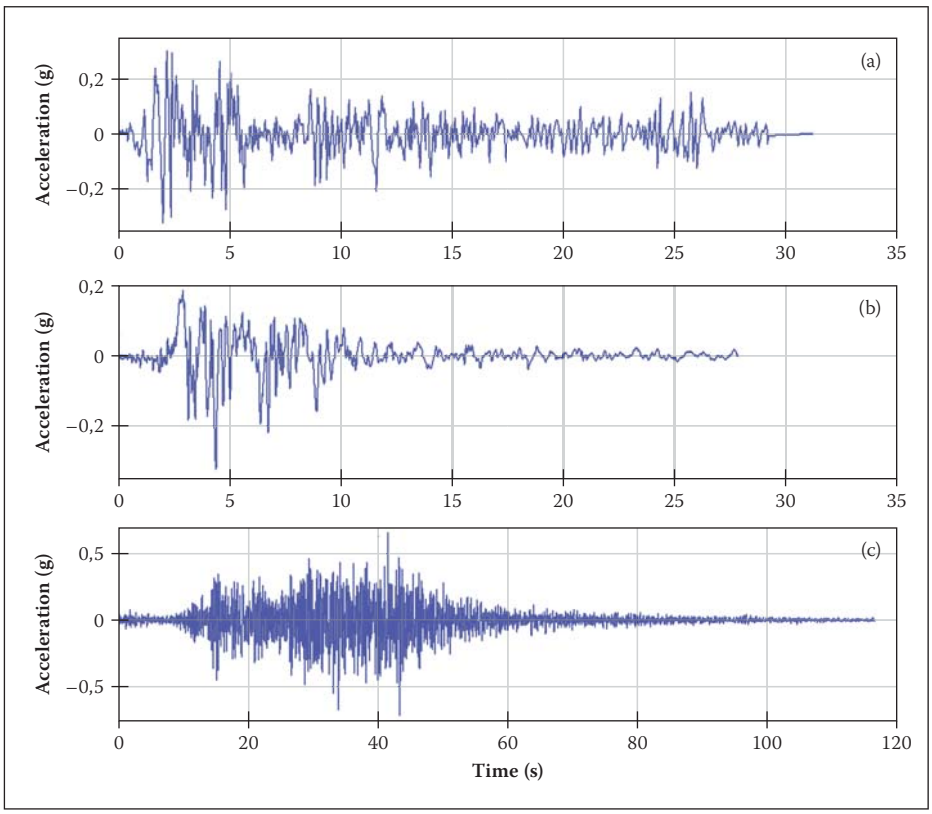

***Figure 1** Acceleration time histories of (a) El Centro earthquake, (b) Northridge earthquake and (c) Llolleo earthquake. Note the different time and acceleration scales*

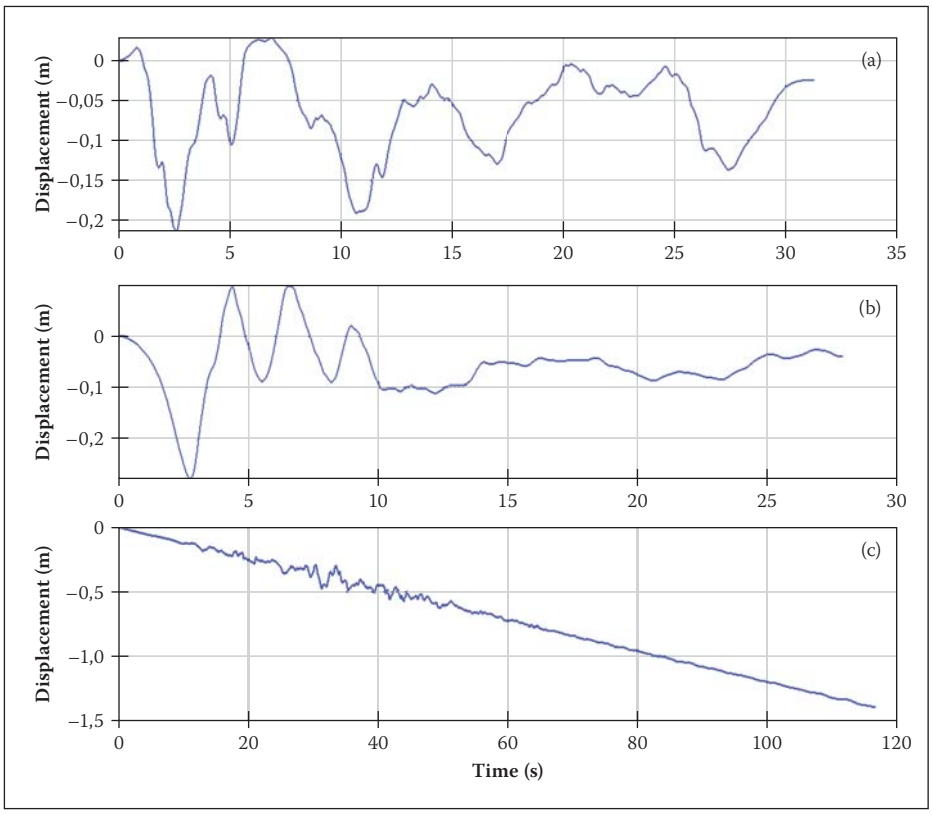

***Figure 2** Displacement time histories of (a) El Centro earthquake, (b) Northridge earthquake and (c) Llolleo earthquake*

response spectra. The filtered earthquake displacement histories are applied to a full-scale, dry-stacked masonry structure and the measured acceleration and displacement results of the shaking table are then presented and analysed. The paper concludes with a brief discussion of how the earthquake tests compare with design response spectra for the full-scale, dry-stacked masonry structure investigated.

SAMPLE EARTHQUAKES

Three earthquakes are considered here: (a) the El Centro earthquake of 1940; (b) the Northridge earthquake of 1994; and (c) the Llolleo earthquake of 1985. The acceleration time histories for these earthquakes are shown in Figure 1. Table 1 gives some statistics of these earthquakes.

EARTHQUAKE TESTING EQUIPMENT

The earthquake simulation was run at the Track Testing Facility of Transnet Freight Rail, Jeppestown, Johannesburg, South Africa (Transnet Facility for short). The servo-hydraulic machine used was the MTS 493 Flex Test GT, driven by four hydraulic pumps supplying 1 000 litres per minute. The displacement time history for each of the earthquakes, derived subsequently, was imported as the control signal. The actuator attached to this machine has a capacity of +/-250 kN and a stroke of +/-75 mm. As will be seen below, the stroke range of 150 mm proved to be the limiting factor in the earthquake test simulations. The actuator was attached to a 4 by 4 m, one degree of freedom shaking table. This shaking table has a natural resonance frequency of 25,6 Hz when fully loaded, which is well above the expected fundamental natural frequency of the test structure. For more details on the shaking table, the reader is referred to reference De Kock (2002) (report reproduced in Ngowi 2006).

DISPLACEMENT HISTORY OF SAMPLE EARTHQUAKES

Since the usual control parameter of servo-hydraulic test machines is displacement and not acceleration, the above acceleration histories were numerically double-integrated to produce the displacement records. It must be pointed out that the computed displacement signals are not necessarily correct; the initial acceleration traces of the earthquakes were below the recording instrument's trigger level; consequently they were not recorded (Chopra 2001) and thus were not double-integrated. However, since the accelerations were small (below the

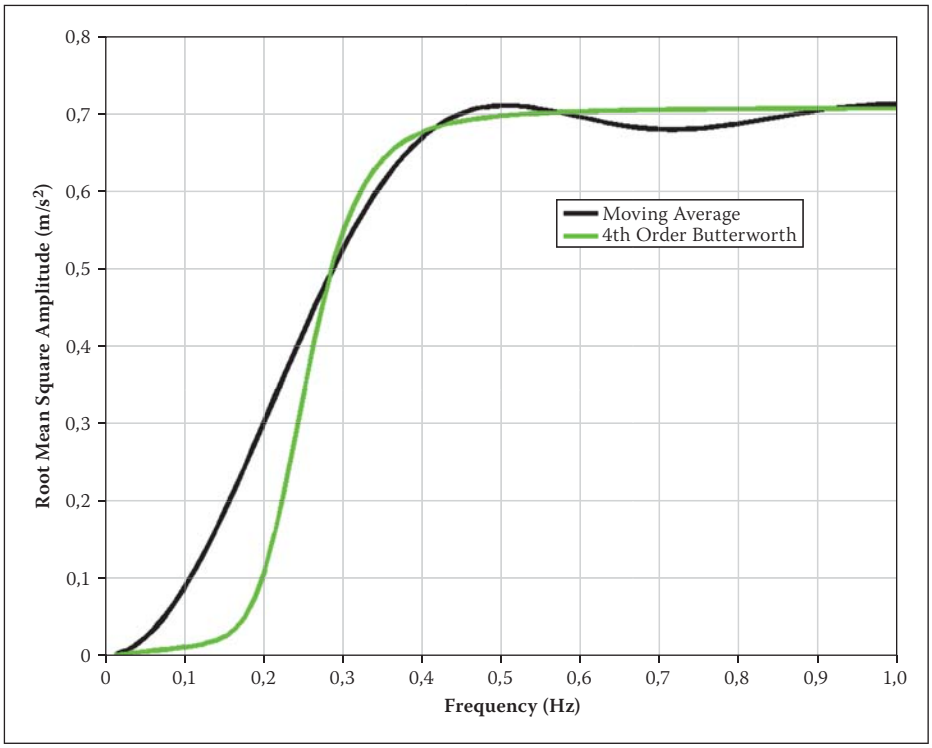

***Figure 3** The effect of the two filters on a harmonic input at different frequencies (i.e. the transfer function of the filters)*

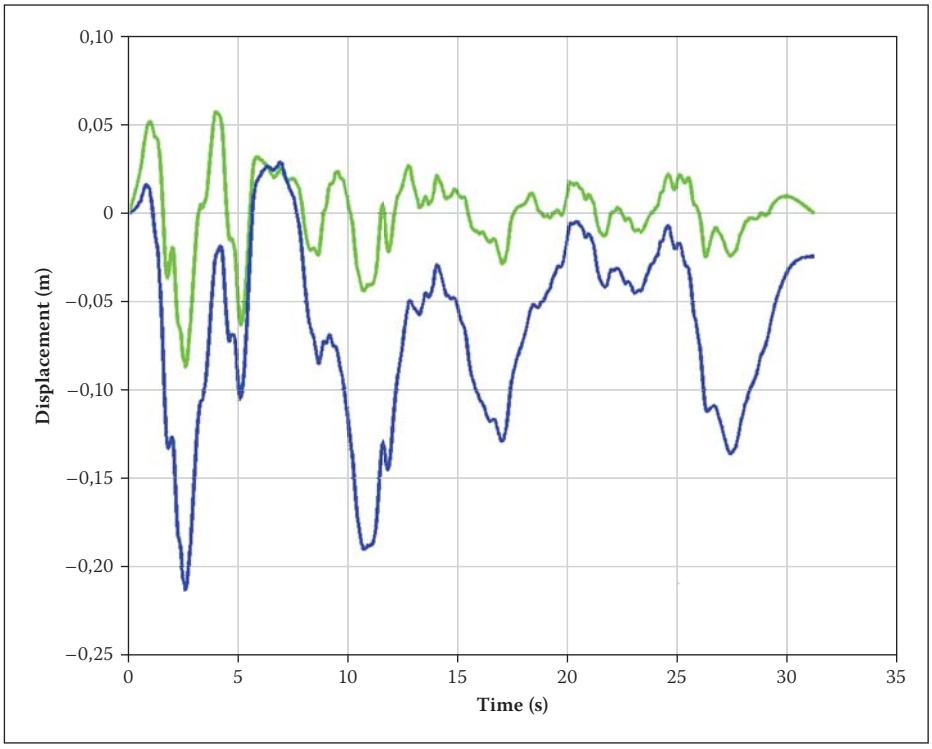

Figure 4 *Unfiltered (blue) and filtered (green) El Centro displacement history*

trigger value), and this paper concentrates on reproducing the recorded earthquakes' acceleration and not the unknown displacement signals, this initial acceleration trace just prior to the earthquake will be ignored. The numerical integration of the acceleration trace was performed using the standard trapezoidal integration rule twice to produce the displacement time histories shown in Figure 2. Although higher-order and more complicated numerical integration schemes could be employed, the trapezoidal rule was chosen for its simplicity and sufficient accuracy.

The Llolleo displacement signal clearly shows an artefact of the numerical integration, namely that any offset, no matter how small, in the original acceleration readings produces an offset and/or a linear signal that is superimposed on the displacement readings. The offset could be real, or due to sensor calibration error. One way to remove this offset is by subtracting it from the original acceleration signal. A second method, which is implemented in this paper, is to filter the data with a high-pass filter.

The range of displacements of each earthquake is large, falling well outside the range of the strokes of standard actuators. The Transnet Facility actuator that was available for these earthquake simulations has only a 150 mm stroke (+75 to –75 mm). Figure 2 shows that the earthquakes' displacements exceed this value, in some instances substantially. To carry out the earthquake tests, the signals shown in Figure 2 had to be processed to fall within the stroke capabilities of the Transnet Facility actuator. This was achieved by high-pass filtering of the displacement signal.

FILTERING THE EARTHQUAKES' DISPLACEMENT HISTORY

The goal of filtering the displacement history is to reduce the displacements to within the maximum stroke of the actuator without substantially changing the overall acceleration history. Although a number of filtering options can be employed to achieve this aim, this paper focuses on two standard methods: (a) the moving average method; and (b) a 4th-order high-pass Butterworth filter method. In digital signal processing, the filtered data (Y_f) are derived from the original data (Y) using a set of simple arithmetic operations:

$$a_1 Y_f(n) = b_1 Y(n) + b_2 Y(n-1) + \ldots + b_{nb+1} Y(n-n_b) - a_2 Y_f(n-1) - a_3 Y_f(n-2) \ldots - a_{na+1} Y_f(n-n_a) \quad (1)$$

where $b_1 \ldots b_{nb+1}$ and $a_1 \ldots a_{na+1}$ are filter coefficients, n is the current data point, n_a is the order of the a filter and n_b is the order of the b filter.

In the moving average filter, $b_1 = b_2 \ldots = b_{nb+1} = 1$ and all the a coefficients are zero, except for a_1 which is set equal to n_b+1 (i.e. the number of points in the moving average). The filtered data (Y_f) are then subtracted from the original signal (Y) to give the moving average filtered displacement, Y_{MA}. The number of points in the moving average is chosen as the minimum number that will reduce the filtered displacement (Y_{MA}) to lie within the bounds of the actuator stroke.

For the 4th-order high-pass Butterworth filter, b_1 to b_5 and a_1 to a_5 are specifically chosen to give a required cut-off frequency (f_c) (Sedra & Smith 1998). Ideally, frequency components of the original data above the cut-off frequency are preserved, while frequency components below the cut-off frequency are eliminated. The filtered displacement (Y_{BW}) is then equal to Y_f. In this case, the smallest cut-off frequency is chosen

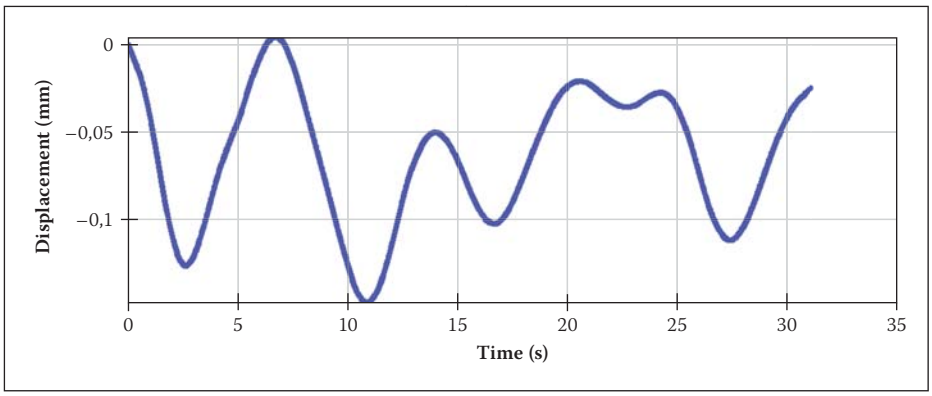

***Figure 5** Moving average curve produced from the El Centro displacement time history with a 2,0 s time window*

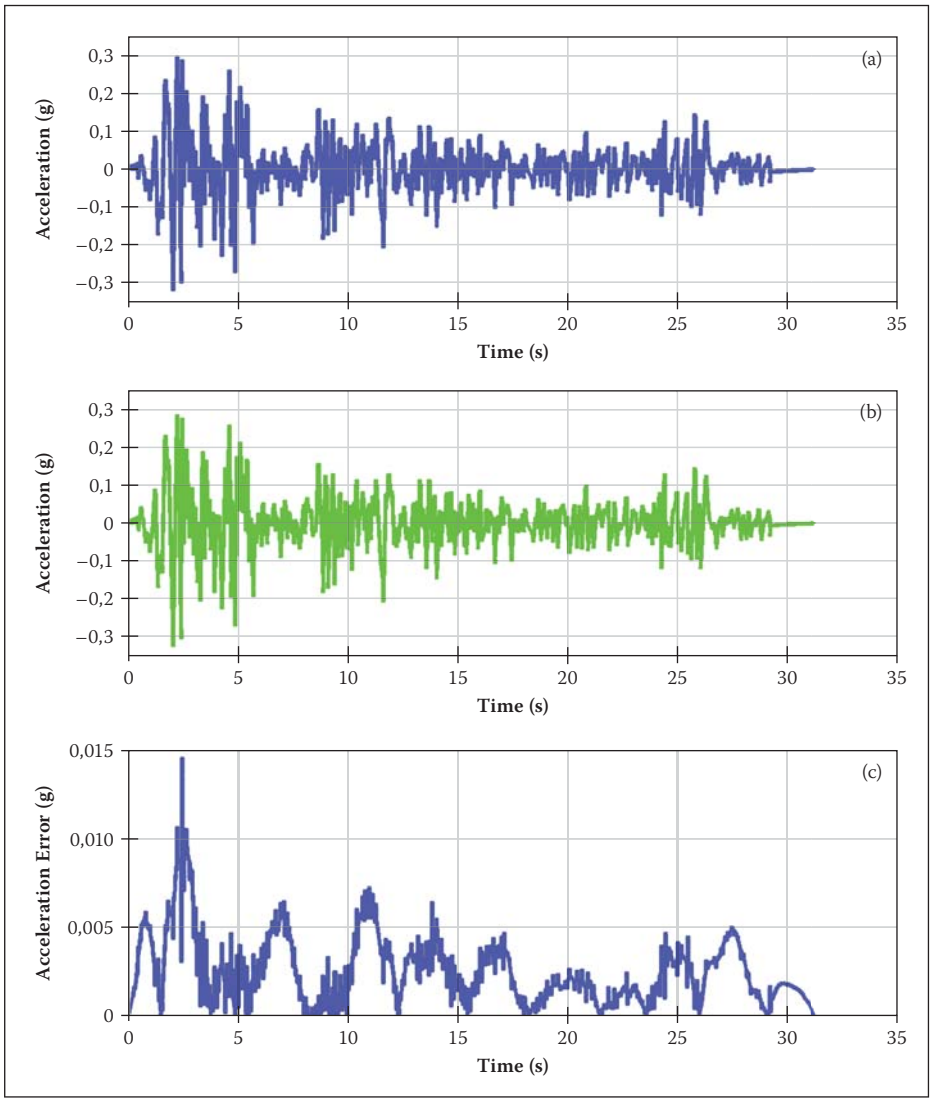

***Figure 6** (a) The original El Centro acceleration time history, (b) the filtered El Centro acceleration history assuming a 2,0 s time window in the moving average filter and (c) the error introduced by considering a filtered El Centro signal with a moving average time window of 2,0 s*

that will reduce the filtered displacement to within the bounds of the actuator stroke.

In general, applying filters introduces a phase or time shift in the filtered versus the original data (consider, for example, filtering using moving averages). One of the standard techniques for reducing or eliminating this time lag is to pass the original data through the filter once in the forwards direction, and then pass the resulting data through the same filter in the backwards direction. The phase shift caused by the first filter pass is cancelled by the second, reverse pass. Here, for this reason, in both the moving average and the 4th-order Butterworth cases, the filtered data ($\underline{Y_f}$) were also passed through the same filters in reverse. All filtering operations were done using MATLAB Version 6.5 (2002). Figure 3 plots the transfer function for the moving average and the 4th-order Butterworth high-pass filters. The cut-off frequency is 0,25 Hz for the Butterworth filter, and the moving average time window is 2 s. As will be seen, applying these filters to the earthquake displacement data ensured that the maximums were within the bounds of the actuator stroke of the Transnet Facility.

The moving average filter applied to the El Centro earthquake

Figure 4 plots the unfiltered and filtered El Centro earthquake displacement history using the moving average approach with a 2,0 s time window.

Figure 5 shows the slowly fluctuating moving average curve with a 2,0 s time window that was subtracted from the El Centro displacement time history Figure 4 (blue curve). From Figure 5 it can be seen that (a) the speed of oscillation is slow – less than 0,2 Hz – and (b) the magnitude of the subtracted signal is large. Due to the filter used (see Figure 3), it is not surprising that the subtracted signal oscillates so slowly. The slowly fluctuating but large signal to be subtracted works towards fitting the displacement history into the MTS servo-hydraulic machine.

A comparison of the filtered and unfiltered displacement histories in Figure 4 reveals several striking points. The filtered data look significantly different from the original displacement history. Not only are the magnitudes different, but also the shape of the curve does not match that of the original signal. The maximum filtered amplitude of the displacement, with a 2,0 s moving average time window, is 57 mm and the minimum is –87 mm. Thus the stroke required is 144 mm, which is less than the 150 mm stroke of the Transnet Facility actuator. The question now arises: how different is the original El Centro acceleration time history from the filtered displacements? To answer this question, the filtered displacement El Centro graph (Figure 4, green curve) is differentiated twice using the standard numerical central difference method. The resulting filtered acceleration graph is subtracted from the original El Centro record, and the absolute value taken. This is the error between the filtered and original data.

$$|\ddot{Y}_f - \ddot{Y}| = error \qquad (2)$$

where $\ddot{Y}_f$ is the filtered displacement signal, Y is the original signal and double dots refer to double differentiation with respect to time.

Figures 6(a) and 6(b) plot the time history of the unfiltered and filtered El Centro accelerations. Filtering is carried out assuming

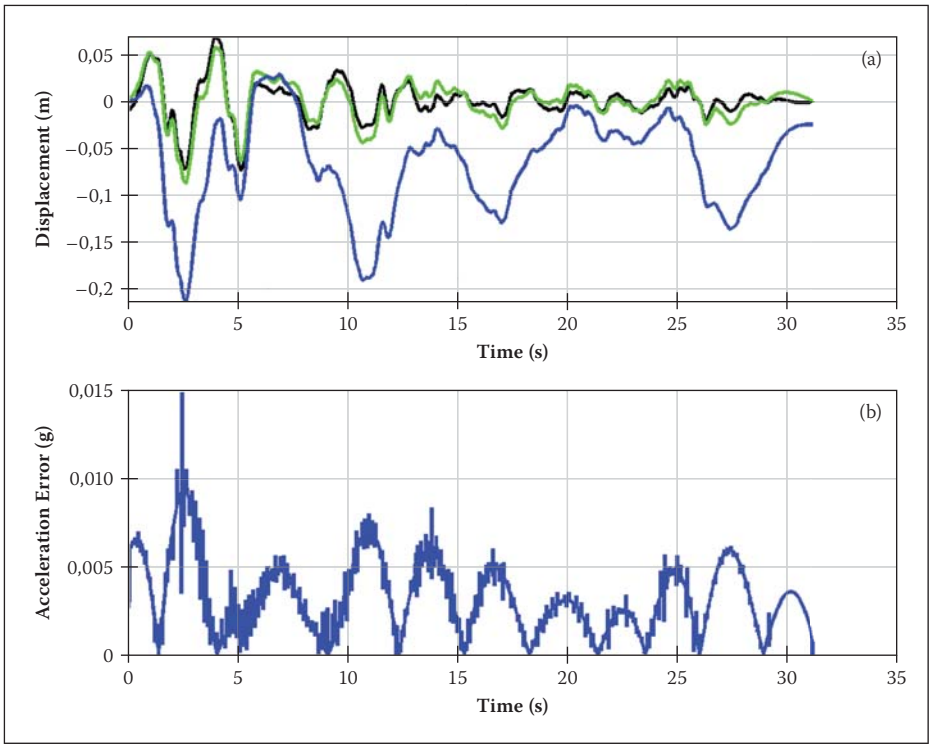

Figure 7 *(a) Filtered El Centro signal with the moving average approach (green line), the 4th-order Butterworth filter using a cut-off frequency of 0,25 Hz (black line) and the unfiltered displacement history (blue line), and (b) the error introduced by considering a filtered El Centro signal with the 4th-order Butterworth filter*

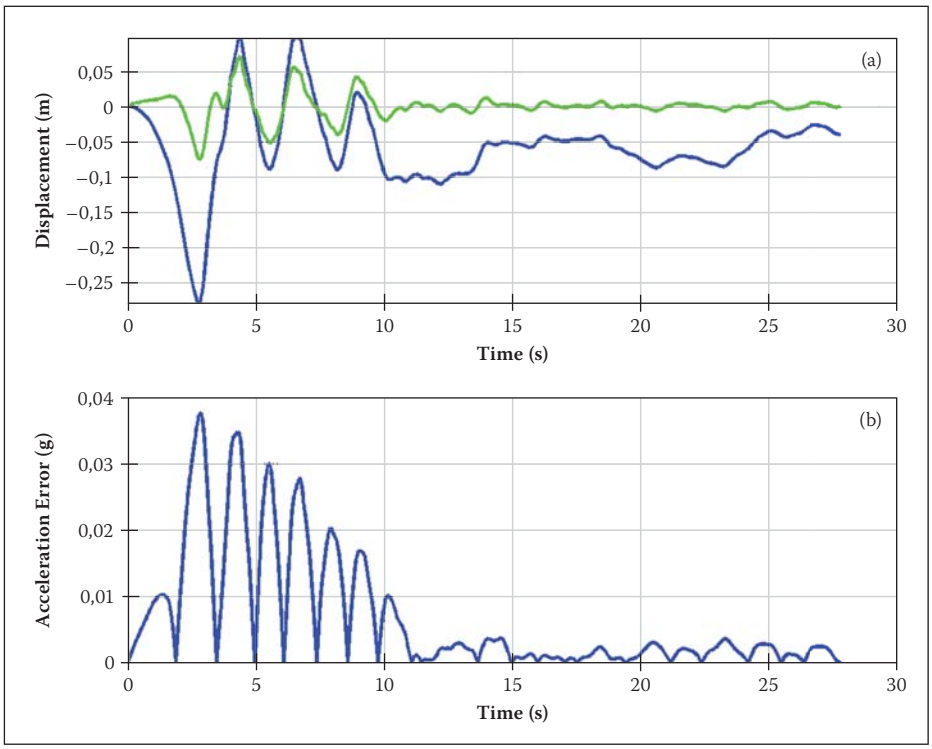

Figure 8 *(a) Northridge earthquake displacement time history filtered using a moving average with a window of 1,125 s (green line) and the unfiltered displacement history (blue line), and (b) the corresponding error in accelerations due to the filtering*

a 2,0 s time window in the moving average. The difference between these two signals, or the error, is plotted in Figure 6(c).

Figure 6(c) shows that the maximum error is 0,0146 g, or 4,6% of the original signal. This maximum error occurs at only one point; the majority of the error is smaller than 0,005 g. The root mean square (RMS) error is only 0,0031 g. Thus it can be concluded that although an error is introduced by filtering the original displacement data, it is relatively small. The main benefit of the filtering is that the overall required stroke of the actuator is now only 144 mm and that can be applied by the Transnet Facility MTS machine.

The 4th-order Butterworth filter applied to the El Centro earthquake

Figure 7(a) plots the filtered El Centro earthquake displacement history using the moving average approach described above, and the 4th-order Butterworth filter with a cut-off frequency of 0,25 Hz. For comparison, the unfiltered time history is also shown. The error for the 4th-order Butterworth filter applied to the El Centro earthquake is computed using eq. 2 to produce Figure 7(b).

The displacement histories produced by the moving average and the 4th-order Butterworth filter are close to each other. This is not surprising since the transfer functions for the two filters are comparable (see Figure 3). The errors in acceleration produced by using the 4th-order Butterworth filter are also very similar (compare Figure 6(c) with Figure 7(b)). The maximum error from Figure 7(b) is 0,0149 g, which corresponds to a 4,7% error. As for the moving average filter, this error occurs only at one point. The maximum displacement of the 4th-order Butterworth filtered signal is 69,3 mm, while the minimum displacement is –73,5 mm, giving a stroke of 142,8 mm.

Due to the similarity of the results from the two filters, the moving average filter, which is the simpler approach, was adopted for the other earthquakes.

The moving average filter applied to Northridge and Llolleo earthquakes

For completeness, Figures 8(a) and 9(a) show the filtered displacement histories for the Northridge and Llolleo earthquakes. The unfiltered displacement for the Northridge earthquake is also shown in Figure 8(a). The unfiltered displacement history for the Llolleo earthquake has a large drift component (see Figure 2(c)) and is thus not included in Figure 9(a) for clarity. The errors in accelerations for these two earthquakes, as computed by eq. 2, are plotted in Figures 8(b) and 9(b). For both earthquakes, the moving average time window was taken as 1,125 s. Table 2 summarises the maximum and minimum displacements for each filtered earthquake, the total stroke, the maximum error due to the filtering, and the moving average time window used.

As can be seen from Table 2, the filter was designed so that the errors are minimised and the total stroke is less than 150 mm – the maximum stroke of the MTS Transnet Facility actuator. The error in the signal is the price that has to be paid if the stroke is limited by the actuator. Since the above displacements are not symmetrical about the zero actuator position, the earthquake signals were offset to the average of the maximum and minimum displacements. To understand how these earthquakes can be

Table 2 *The stroke of the filtered earthquake and the maximum error in the signal*

Earthquake	Maximum displacement (mm)	Minimum displacement (mm)	Total stroke (mm)	Maximum error (%)	Moving average time window (s)
El Centro	57	-87	144	4,6	2,0
Northridge	70,1	-75,2	145,3	11,9	1,125
Llolleo	59,3	-49,5	108,8	3,5	1,125

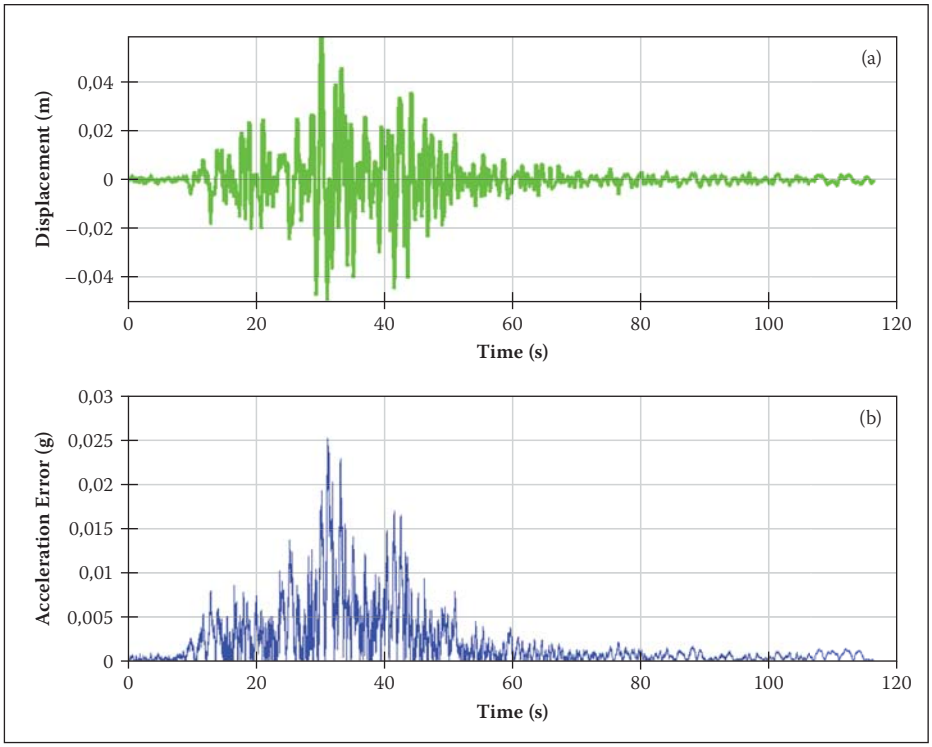

Figure 9 *(a) Llolleo earthquake displacement time history filtered using a moving average with a window of 1,125 s and (b) the corresponding error in accelerations due to the filtering*

used in the design-testing process, the earthquake design spectra have to be considered.

EARTHQUAKE DESIGN SPECTRA

Earthquake response spectrum analysis is an approximate method that allows the structural engineer to design a building in a seismic zone using ***equivalent static forces***. This simplified method assumes the structure to possess a single degree of freedom (Figure 10) and uses only the maximum structural response.

A response spectrum is generated as follows:

1. Obtain the earth acceleration ($A_g(t)$) time history (either measured from an earthquake or calculated).
2. Select a damping ratio (ζ) for a single-degree-of-freedom system (usually taken as 5% if the value is unknown).
3. Select an undamped natural frequency of the structure (ω); where $\omega = \sqrt{k/m}$ with k the structure's stiffness and m the mass (see Figure 10).
4. Calculate the relative displacement response time history ($x(t)$) of the single-degree-of-freedom structure to the ground acceleration by solving the equation:

$$\ddot{x}(t) + 2\zeta\omega\dot{x}(t) + \omega^2 x(t) = -A_g(t) \qquad (3)$$

where the double dot refers to differentiation with respect to time.

5. The displacement response spectrum (S_d) at a natural period of the structure $T_n = 2\pi/\omega$ is given as the *maximum* structural displacement calculated from (4) above.
6. Repeat steps 4 and 5 to calculate the displacement response spectrum over a range of T_n.

The resulting graph of S_d against T_n is called the "earthquake displacement response spectrum". This response spectrum is then used as follows:

1. Estimate the fundamental natural period (T_n) of the structure to be designed and the damping ratio (ζ).
2. Find the maximum displacement response spectrum S_d for the particular T_n and ζ.
3. The maximum force in the structure can then be calculated by:

$$F_{max} = kS_d \qquad (4)$$

where k is the stiffness of the structure.

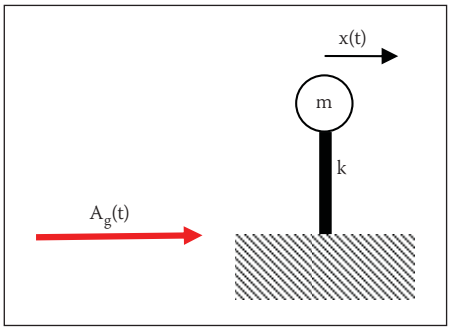

Figure 10 *System whereby the structure is considered as a single degree of freedom*

The estimation of the structural stiffness (k) can often be difficult for the designer. It is thus more convenient to rewrite:

$$F_{max} = m\omega^2 S_d = mS_a \qquad (5)$$

where m is the mass of the structure. S_a is the pseudo-acceleration response spectrum of the structure, given by:

$$S_a = \omega^2 S_d \qquad (6)$$

It should be noted that the pseudo-acceleration response spectrum is not the true acceleration response spectrum. (The true acceleration response spectrum is defined as the peak response acceleration experienced by a structure of natural period T_n for a given earthquake.)

The design codes, such as UBC-97 (Uniform Building Code 1997), typically specify the pseudo-acceleration response spectrum. This design spectrum is the conservative envelope of several response spectra for a set of measured earthquakes. The magnitude of the design earthquake is dependent on several factors, such as the seismicity of the region where the structure is to be built, the underlying soil conditions and the distance of the building to the closest seismic source.

For illustration purposes, the design spectra for three design earthquakes, as specified in UBC-97, will be generated. These three earthquakes correspond to:

I. A small earthquake in a zone of low seismicity (Zone 2A) with the soil profile being hard rock
II. An earthquake in Zone 2, with the soil profile being very dense soil and soft rock
III. An earthquake in Zone 4, with the soil profile being stiff soil and the seismic source being 10 km away and capable of events of large magnitude

The UBC-97 design response spectra are compared with the El Centro, Northridge and Llolleo earthquakes. Both the original and the filtered signals for these three earthquakes will be used to compute the response

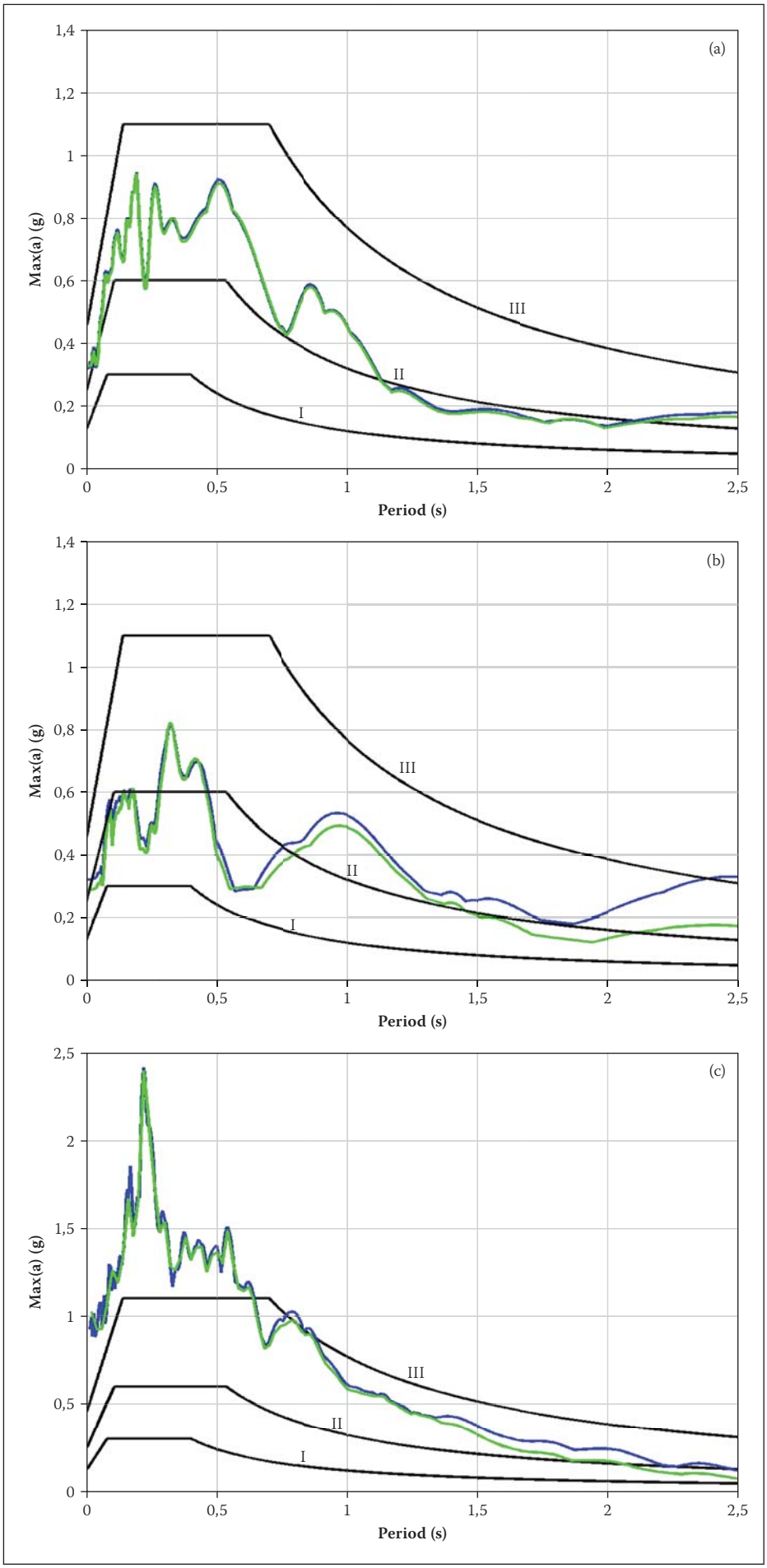

Figure 11 *Response spectra for (a) El Centro, (b) Northridge and (c) Llolleo. The lines correspond to the original earthquake signals (blue) and the filtered signals (green). The black lines are the UBC-97 design spectrum earthquakes*

spectrum using the algorithm presented above, with an assumed damping ratio of 5%. Note that to obtain the input accelerations, the filtered earthquake displacement signals are numerically double-differentiated, using the central difference method. The results are shown in Figure 11.

Figure 11 shows the pseudo-acceleration spectra for the filtered and unfiltered ground accelerations for all three earthquakes. The match is very good when the period of the structure is low (below 1 s). As the period increases above approximately 1 s, the filtered signal starts to under-predict the unfiltered spectrum. This is not surprising since the low-frequency components (or high-period components) have been removed from the original accelerations by high-pass filtering. Figure 11 also shows that the three earthquakes' spectra can be higher than one portion of the design spectrum and lower than another. Where the earthquake's spectrum is higher than the design spectrum, the loading due to the test earthquake is conservative (higher than code requirements). Where the test earthquake's spectrum is lower, the test earthquake is unconservative compared with the code (less than required by the code).

SYNTHETIC EARTHQUAKES APPLIED TO A DRY-STACKED MASONRY STRUCTURE

Since this paper concentrates on earthquake testing and the design code loads, only a brief description of the test structure is given here. The instrumentation, the results from the sensors and the associated discussion are not presented at all. These topics have been presented in a separate publication (see Elvin & Elvin 2008).

Description of the test structure

A full-scale 3,9 by 3,9 m dry-stacked masonry structure, 2,76 m high (shown in Figure 12) was built on the shaking table. This structure corresponds to a single room, built according to Hydraform (2009) and described in Elvin and Elvin (2008). Two standard doorways were introduced on adjacent walls; the other two walls had full-sized windows (1,022 m wide by 0,949 m high). The second door was included as a conservative measure to weaken the structure.

The inside of the masonry structure, as well as the top portion of the outside (see Figure 12), was skimmed with a thin (5 mm) layer of painted plaster. Since the test structure was to be used as a residential dwelling, this was a realistic addition to the structure. The plaster also served as a useful identifier of where cracking or damage occurred during the testing.

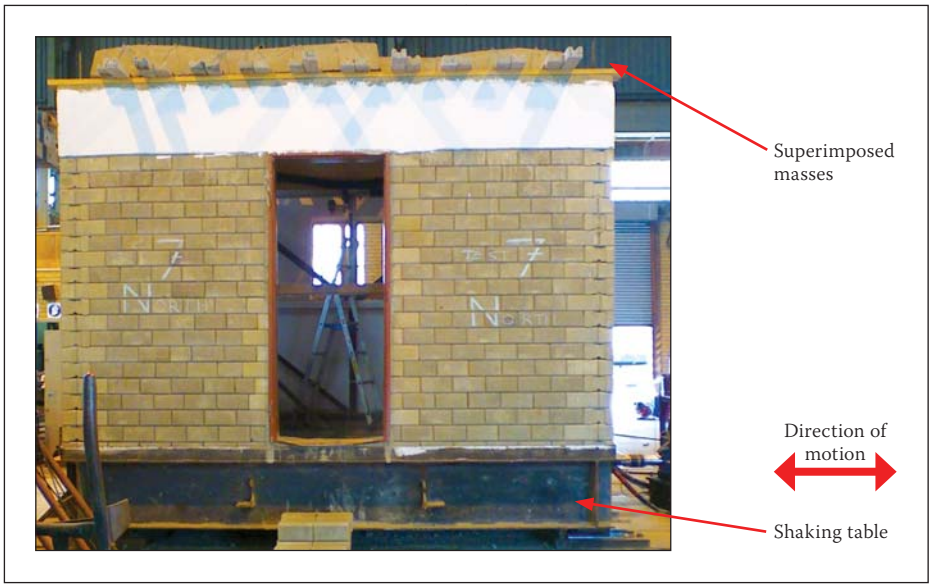

Figure 12 *Test structure and shaking table showing the direction of the base excitation*

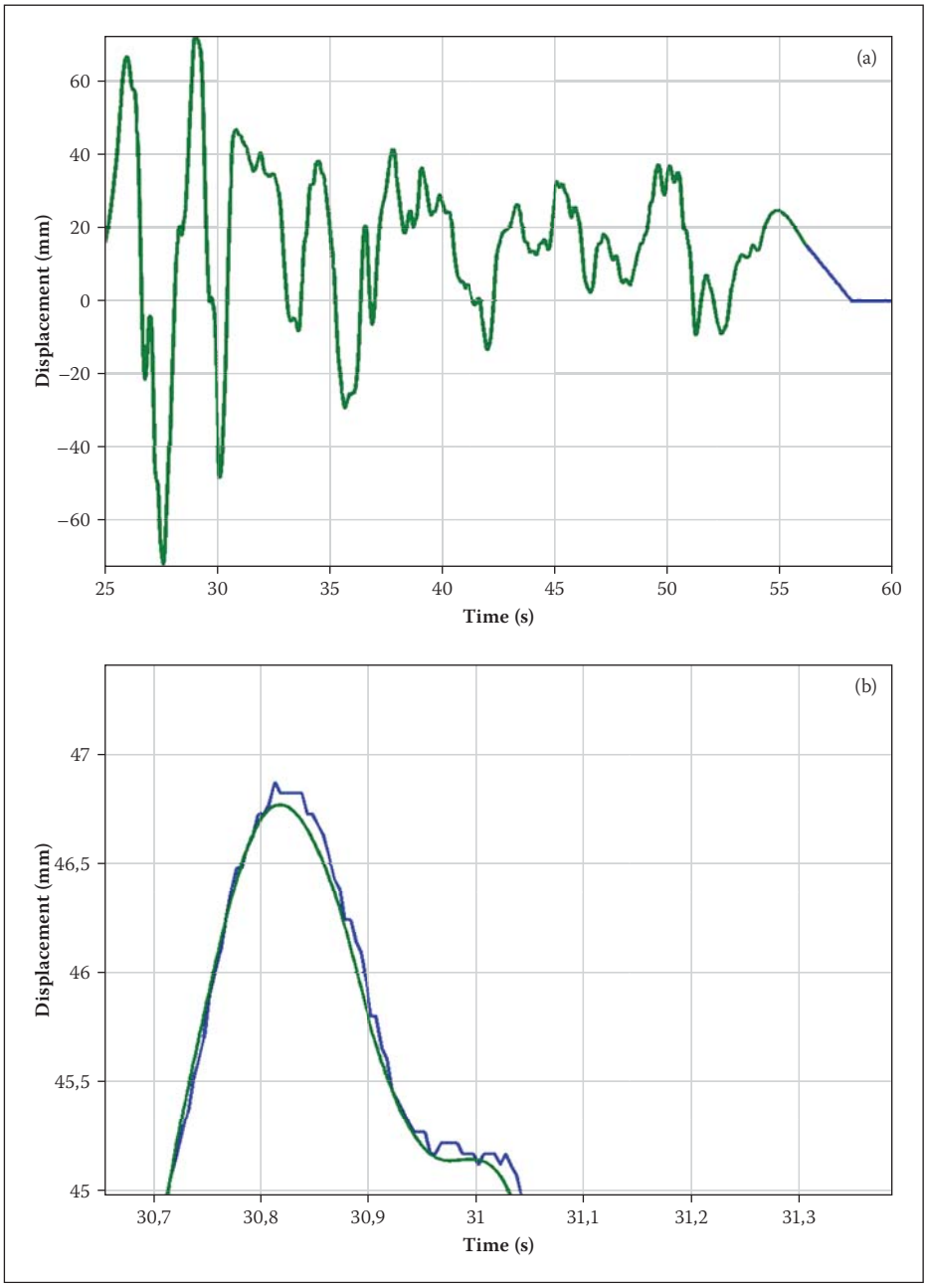

Figure 13 *El Centro Earthquake: (a) the displacement of the shaking table (blue) and the control command curve (green) and (b) zoomed-in view of the command and measured displacements showing that the two are not identical*

The 7 MPa bricks (Hydraform 2009) used in the structure have interlocking keys on two of their sides, as well as a conduit space for reinforcement bars and mortar. In the test structure, the interlocking bricks were dry-stacked and only minimal reinforcement was used (see Elvin & Elvin 2008 for details).

To simulate the foundation, the bottom layer of bricks was laid in a steel channel welded to the shaking table. No roof was included in the structure, and instead concrete masses totalling 2 560 kg were placed on top of the structure. These masses rested freely on the walls (Figure 12), and precompressed the dry-stack masonry, thus stabilising the structure. On the other hand, placing such a large mass as far from the support as possible produced a very unconservative earthquake loading scenario.

EARTHQUAKES APPLIED

The MTS servo-hydraulic machine applied the filtered displacement time histories of the various earthquakes (see Figures 4(b), 8(a) and 9(a)). These displacement time histories constituted the control signals. To determine how accurately the earthquake displacements were being applied by the MTS controller, two sets of sensor readings were taken. The position of the shaking table with respect to a fixed datum was measured by a Linear Variable Displacement Transducer (LVDT). A wireless accelerometer sensor (3DPebble, ZeroPoint Technology 2009) was attached to the shaking table and the base accelerations were recorded.

Typical displacement results are shown in Figure 13 which plots the command (what the plot should be) and LVDT measurements (actual) that the shaking table underwent in the El Centro earthquake simulation. Note that the measured and command displacements are not identical (Figure 13(b)).

The errors in the applied earthquake displacements, which are reported in Table 3, are small, especially compared with the full stroke of 150 mm.

Table 3 *Errors between the control and measured displacements*

Earthquake	Maximum absolute error (mm)	RMS error (mm)
El Centro	0,73	0,14
Northridge	0,79	0,12
Llolleo	2,61	0,23

Although the errors in the displacements are very small, the errors in the accelerations are

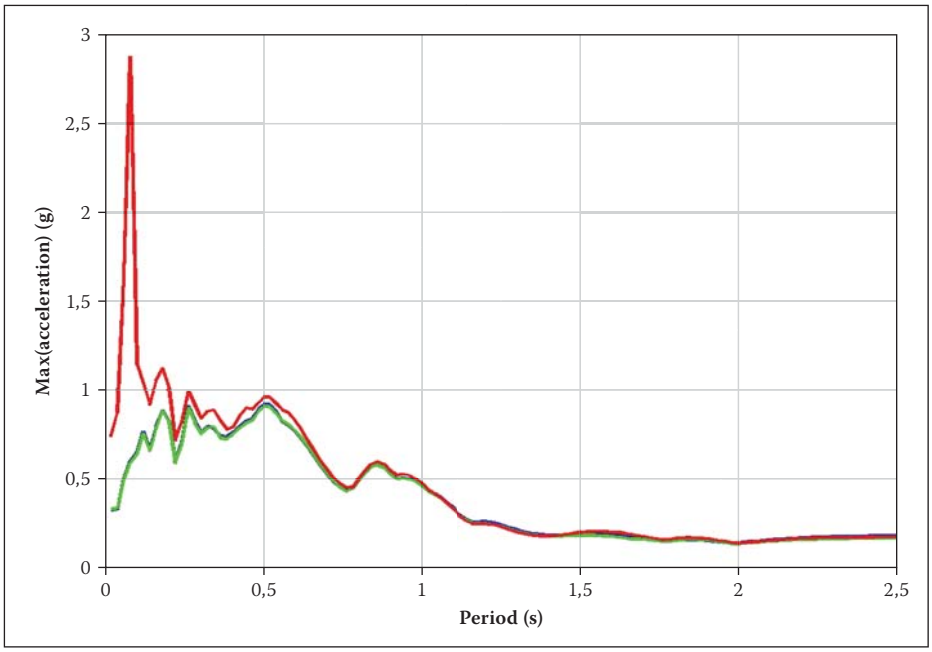

Figure 14 *Response spectra for El Centro. The lines correspond to the original accelerations (blue), the theoretical filtered accelerations (green), and the actual applied accelerations (red)*

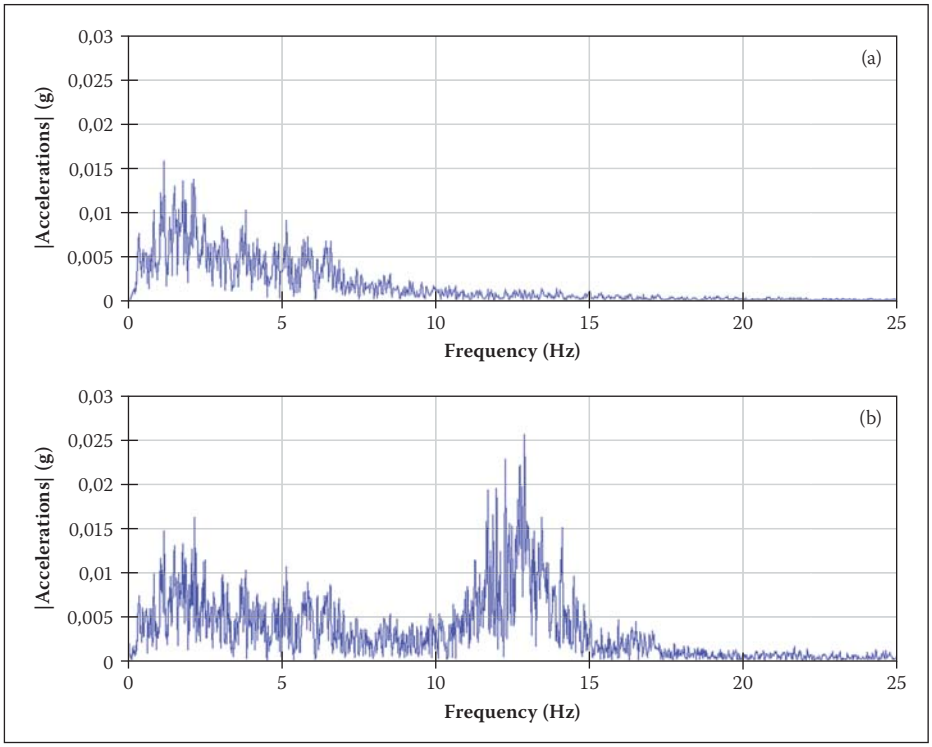

Figure 15 *Fast Fourier transform of accelerations for the El Centro earthquake: (a) derived from the filtered control displacements and (b) measured shaking table motion*

much larger (see Table 4). This is due to the fact that the MTS servo-hydraulic machine control was based on displacements and not accelerations. Any error in the controlled shaking table displacement (see for example the jitter in Figure 13(b)) is amplified in the table's accelerations.

The control acceleration time history was obtained by numerically double-differentiating the filtered displacements using the central difference method. The measured accelerations were shifted in both time and acceleration to match the control accelerations.

Table 4 *Approximate errors between the control and measured accelerations*

Earthquake	RMS error (g)	RMS error as % of max. acceleration
El Centro	0.0212	6.56%
Northridge	0.0134	4.65%
Llolleo	0.0441	6.20%

What is the effect of the error in the measured earthquake accelerations? To answer this question, the response spectra are developed for each sample earthquake, with the input being the actual applied base accelerations which were measured during the experiment. One such spectrum for the El Centro earthquake is shown in Figure 14.

Figure 14 shows that at high periods (low frequencies), the response spectra from the actual applied accelerations and the filtered earthquake accelerations are very similar. At low periods (higher frequencies), the actual applied accelerations produce larger values in the response spectra. Thus the applied base accelerations load the test structure to a greater extent than either the filtered or the original earthquake. The ramifications of the actual applied accelerations on the dry-stacked masonry structure that was tested are discussed in the next section.

At a period of approximately 0,08 s, or 13 Hz, all three response spectra derived with the input being the actual applied base accelerations exhibit a pronounced peak. This peak is due to noise introduced by the MTS servo-hydraulic system, i.e. the servo-hydraulic machine in the experimental set-up used operates with an ever-present superimposed noise, centred at about 13 Hz. The resulting pronounced peak is due to (a) a non-negligible cyclical acceleration due to machine noise, and (b) 13 Hz being a relatively large value which is then squared in eq. (6) to compute the response spectrum. To prove this, Figure 15 plots the fast Fourier transforms of the El Centro accelerations (a) derived from the filtered control displacement signal, i.e. the synthetic earthquake, and (b) the actual measured motion of the shaking table. Up to approximately 7 Hz, the control and the measured acceleration frequency contents are very similar. Beyond this frequency, the filtered El Centro signal does not have any dominant components. The measured accelerations, however, have a large peak around 13 Hz. This shows that the MTS servo-hydraulic machine introduces this frequency noise into the displacements and accelerations.

LOAD TESTING VERSUS DESIGN CODE REQUIREMENTS

The dry-stacked masonry test structure was subjected to a number of earthquakes. How does this loading compare with the design code requirements? The answer to this question is: if the response spectrum for the test earthquake is equal to, or larger than, the requirements from the code's design response spectrum, ***at the natural period of the structure***, then the structure is adequately loaded by the test earthquake. Of course, the response spectrum for the test earthquake could be well above the design requirement,

rendering the loading over-conservative. In this case, the input test earthquakes can be scaled down (e.g. ½ or 1 x El Centro earthquake), reducing the measured response spectrum to the code at the natural period of the structure. Peaks and elevated levels in the measured response spectra due to equipment limitations (such as the effects of machine noise) are more difficult to reduce.

Figure 11, for example, shows several design response spectra for earthquakes of various magnitudes. The natural frequency of the dry-stacked masonry test structure is approximately 5 Hz (Mofana & Rathebe 2005) or it has a natural period of 0,2 s. Figure 11 shows that for a period of 0,2 s, the test earthquakes used have a peak and could be well above the design spectra for the test structure. For the 0,2 s period, the Llolleo earthquake applied is, in fact, almost two times the loading magnitude requirement of a large synthetic design spectrum of earthquake III (as constructed using UBC-97, see Figure 11(c)). Thus it can be concluded that due to the low natural period of the dry-stacked masonry structure investigated, the earthquake loads tests are on the conservative side.

It must be emphasised that the code response spectra are constructed assuming elastic structural behaviour. However, these response spectra are used for both linear and non-linear behaviour (see, for example, Magliulo et al 2007). Further, the test structure's behaviour and the damage accumulation (non-linearity) can be monitored throughout the earthquake test and then classified, e.g. by using the European Macroseismic Scale (EMS) (EMS-98, see Grunthal 1998).

CONCLUSION

This paper has described a method of filtering earthquakes to overcome limitations in the testing equipment. The method of comparing the applied earthquakes to design code requirements has also been presented.

It is concluded that removing the low-frequency components of the applied acceleration and displacement time histories has little effect on the response of the structure as the components removed are sufficiently far from its natural frequency. Removing the low-frequency components does reduce the applied displacement. The filtering has a larger effect on the displacement than on the accelerations, where higher frequencies are emphasised.

Three earthquakes were considered: El Centro, Northridge and Llolleo. The acceleration signals from these earthquakes were numerically double-integrated to produce a displacement time history. The displacements that were required to achieve these earthquakes were beyond the stroke range of the Transnet Facility MTS servo-hydraulic test system available. The displacement earthquake signals were filtered to remove the slow-varying components. Two filters were investigated: the moving average and the 4th-order Butterworth high-pass filter. It was found that they both produced very similar results, and the simpler moving average approach was adopted. The filtering reduced the maximum to minimum stroke required. Although the slowly fluctuating part of the signal was lost, the filtered displacements fitted into the stroke of the servo-hydraulic machine. The maximum peak error in accelerations introduced into the signal by filtering was computed and found to be 11,9% (at one point); the worst root mean square error was less than 3,4% of the maximum acceleration.

A full-scale dry-stacked masonry structure built on a one-degree-of-freedom shaking table, utilising interlocking bricks, was subjected to the three filtered earthquakes. The measured shaking table displacements were close to the filtered, derived earthquakes. The measured acceleration of the shaking table, on the other hand, showed a root mean square error of 6,56% when compared with the filtered earthquake acceleration time history. A significant source of error was that control was based on displacement and not acceleration. A second source of error was the noise, centred at approximately 13 Hz, introduced by the MTS servo-hydraulic machine itself.

The response spectra for the various earthquakes were computed and compared with specific case design response spectra calculated from UBC-97. It was found that at low periods, the applied earthquakes can be above the design spectra (which is conservative), and at high periods below them (which is unconservative). This is dependent on the design earthquake's size and location. The dry-stacked masonry structure tested has a natural period of approximately 0,2 s; at this period, the applied test earthquakes could be well above the design response spectrum for the test structure.

It must be emphasised that the filter settings have to be selected carefully and are specific to the structure being tested. For the dry-stacked masonry structure considered, the frequency components below 0,25 Hz (or above a 4 s period) were filtered out. This results in the filtered response spectra deviating from the unfiltered ones above a period of approximately 1,5 to 2 s. In the present case, this is well above the 0,2 s fundamental period of the test structure.

When structures are being tested under simulated earthquake base excitation, it is important to consider the limitations of the testing equipment in terms of the actuator's stroke and load capacity. The control characteristics of the servo-hydraulic machine have to be taken into account; acceleration control might not be feasible or might be too difficult to implement. The frequency components of the ground excitation have to be determined and the actuator has to be able to provide the required input accelerations over the spectral range of the earthquake. It must be pointed out that high-frequency loading might not be possible with many servo-hydraulic testing machines. For all these reasons, correct filtering of the signal is important to preserve the required frequency content of the earthquake. As has been shown in this paper, high-frequency noise or jitter in the servo-hydraulic system can produce very severe loading conditions for stiff structures – well above the design response spectra.

ACKNOWLEDGEMENTS

This research was funded in part by the NRF, under grant IFR2008051900016, and partly by Hydraform Holdings. The use of the Track Testing Facility of Transnet Freight Rail, Jeppestown, South Africa, is appreciated. The technical assistance of Josia Meyer and Chris de Jongh, both of the Transnet Facility, is gratefully acknowledged. The Hydraform Group is thanked for building the test structure. In particular, the technical help of John Roxburgh and Quintin Booysen of Hydraform is gratefully acknowledged. A special tribute is paid to the late Andrew Hofmeyer for his setting up of the entire original instrumentation system.

REFERENCES

3DPebble Wireless Accelerometer sensor 2009. ZeroPoint Technology, http://www.zeropnt.com.

Chopra, A K 2001. Dynamics of structures: theory and application to earthquake engineering. 2nd edition. Upper Saddle River, New Jersey: Prentice Hall, p 203.

De Kock, M J 2002. Conceptual design of vibration table for testing of brick structures. Report M57-276.02, Megmet (Pty) Ltd.

Elvin, A A & Elvin, N G 2008. Experimental earthquake loading of a full-scale dry-stacked masonry structure. Report for Hydraform Holdings (Pty) Ltd.

Grunthal, G (ed) 1998. European Macroseismic Scale, EMS-98.

Griffith, M C, Lam, N, Wilson, J L & Doherty, K 2004. Experimental investigation of unreinforced brick masonry walls in flexure. *J Struct Engng, ASCE*, 130(3):423–432.

Hydraform, 2009, Hydraform Holdings (Pty), Ltd., http://www.hydraform.com/files/english_manual.pdf

Magliulo, G, Maddaloni, G & Cosenza, E 2007. Comparison between non-linear dynamic analysis performed according to EC8 and elastic and

non-linear static analyses. *Engineering Structures*, 11:2893–2900.

MATLAB, Version 6.5, 2002. Mathworks Inc., Nantucket, MA, USA.

Mofana, N C and Rathebe, T K 2005. Dynamic response of masonry structures, BSc thesis, University of the Witwatersrand, Johannesburg, South Africa.

Ngowi, J 2006. Stability of dry-stack masonry. PhD thesis, University of the Witwatersrand, Johannesburg, South Africa.

Saunders, I 2005. South African National Seismograph Network (SANSN). FSDN Report 2005, Council for Geoscience, http://www.fdsn.org/FDSNmeetings/2005/South_Africa_FDSN_2005.pdf

Sedra, A S & Smith, K C 1998. Microelectronics circuits, 4th edition. UK: Oxford University Press, p 893.

Uniform Building Code 1997. Volume 2. Structural engineering design provisions. International Conference of Building Officials, Whittier, California.

ADDENDUM

JOURNAL OF THE SOUTH AFRICAN INSTITUTION OF CIVIL ENGINEERING

Vol 51 No 2, 2009, Page 30, Addendum to Paper 689

Experimentally applied earthquakes and associated loading on a full-scale dry-stacked masonry structure

A Elvin

The following is an addendum to the above-mentioned paper which was published in the *Journal of the Souh African Institution of Civil Engineering*, 51(1) 2009, pp 15–25

ADDENDUM TO ACKNOWLEDGEMENTS (PAGE 24):

The research reported in the above-mentioned paper was carried out on the shake table and system envisioned, implemented and spearheaded by Prof H Uzoegbo of the University of the Witwatersrand. He also allowed us to use the masonry structure for testing. His contribution is gratefully acknowledged.

Prof A Elvin (author)